LARGE-EDDY SIMULATION OF AN ELECTRONIC SYSTEM FLOW

Yongmann M. Chung and Paul G. Tucker
Fluid Dynamics Research Centre
Department of Engineering, University of Warwick
Coventry CV4 7AL, United Kingdom
Y.M.Chung@warwick.ac.uk, P.G.Tucker@warwick.ac.uk

ABSTRACT

The turbulent flow and heat transfer inside an electronic system is computed with large-eddy simulation (LES) using three subgrid-scale models. The flow is highly oscillatory and flow separation takes place in several regions. Accurate prediction of the internal turbulent flow and thermal fields is important in the cooling of electronics. The one-equation linear subgrid-scale (SGS) model of Yoshizawa and the non-linear SGS model of Kosović as well as the Smagorinsky model are used to calculate the residual stress tensor. The results are compared with Laser Doppler Anemometry (LDA) measurements along with Unsteady Reynolds Averaged Navier-Stokes (URANS) computations. The LES convincingly reproduces a highly oscillatory turbulent flow. Compared to URANS predictions, the LES results give better agreement with turbulence measurements. The one-equation subgrid-scale models produces better results than the Smagorinsky model in terms of heat transfer.

INTRODUCTION

As the demand for compact, high performance electronic systems increases, cooling is becoming an ever-increasing issue. Generally, electronic systems contain many circuit boards and internal geometries can have numerous corners and recesses (see Fig. 1). These geometrical features can cause abrupt changes in flow direction, separation and consequently large-scale vortices. The subsequent convection of vortices gives rise to significant flow unsteadiness and consequently temporal heat transfer variations (Chung *et al.*, 2003).

Most previous electronic related simulations are laminar or URANS (Unsteady Reynolds-averaged Navier-Stokes) based. Unsteady fluid flow and heat transfer in grooved channel (Ghaddar *et al.*, 1986a) and sharp 180° bend (Chung *et al.*, 2003) flows of especial relevance to electronic systems have been studied. Grooved channel flow is a model for the idealised two dimensional isothermal cyclic flow in channels with IC (Integrated Circuit) like protrusions. Ghaddar *et al.* (1986b) and and Patera and Mikic (1986) use two dimensional non-isothermal predictions to illustrate the potential for heat transfer enhancement using the unsteadiness observed by Ghaddar *et al.* (1986a). Chung *et al.* (2003) show a neglected electronics cooling relevant geometry is the low Reynolds flow round a sharp 180° bend (see Fig. 2). This is a prototype for flow turned around circuit boards and is also found in the electronics cooling paper of Chung, Tucker and Luo (2001). Chung *et al.* (2003) show that for $Re > 600$ the flow becomes unsteady. Then, as in the grooved channel dramatic increases in heat transfer are found. Tucker (2001) applied several turbulence models to the geometry shown in Fig. 1 with limited success. Many turbulence models could not reproduce the experimentally observed strong flow oscillations. The flow complexity makes accurate URANS simulations difficult. Generally, URANS simulations with linear and nonlinear turbulence models under-predicted the turbulence intensities (Tucker *et al.*, 2003).

Electronic system flows are in a sense well suited to large-eddy simulation (Rollet-Miet *et al.*, 1999). This is because relative to RANS turbulence models, the subgrid-scale model used in LES is less sensitive to the mean flow (Ferziger, 1993; Lesieur and Métais, 1996; Rodi *et al.*, 1997; Jiménez and Moser, 2000). Recently, a large-eddy simulation for this geometry was performed by Chung *et al.* (2001). Compared to URANS predictions, the LES with the Smagorinsky model gave better agreement with turbulence measurements. However, the average error was still large.

In this study, LES with two one-equation subgrid-scale models is performed for the flow inside an idealised electronic system. The geometry consists of three main hollow block-like components, defined as regions 1, 2 and 3. Regions 1 and 2 have fans attached to them. Details of the flow configuration can be found in Fig. 1. Simulation results are compared with LDA data of Tucker and Pan (2001).

NUMERICAL METHODS

LES methodology

In LES only the large-scales are resolved and the small-scales are modelled. Governing equations of LES are the filtered incompressible Navier-Stokes and continuity equations:

$$\frac{\partial \overline{u}_i}{\partial t} + \frac{\partial}{\partial x_j}(\overline{u}_i \overline{u}_j) = -\frac{\partial \overline{p}}{\partial x_i} - \frac{\partial}{\partial x_j}\tau_{ij} + \nu \frac{\partial^2 \overline{u}_i}{\partial x_j^2}, \qquad (1)$$

$$\frac{\partial \overline{u}_i}{\partial x_i} = 0, \qquad (2)$$

where the overbar denotes the filtering operation. In these equations, u_i are the velocity components, τ_{ij} is the residual stress tensor and ν is the molecular viscosity.

In this study, three subgrid-scale models are used to calculate the residual stress tensor,

$$\tau_{ij} = \overline{u_i u_j} - \overline{u}_i \overline{u}_j. \qquad (3)$$

The anisotropic components of τ_{ij} is defined as σ_{ij}.

Smagorinsky model.

In the Smagorinsky model, the eddy viscosity ν_t is obtained by assuming that the small-scales are in equilibrium.

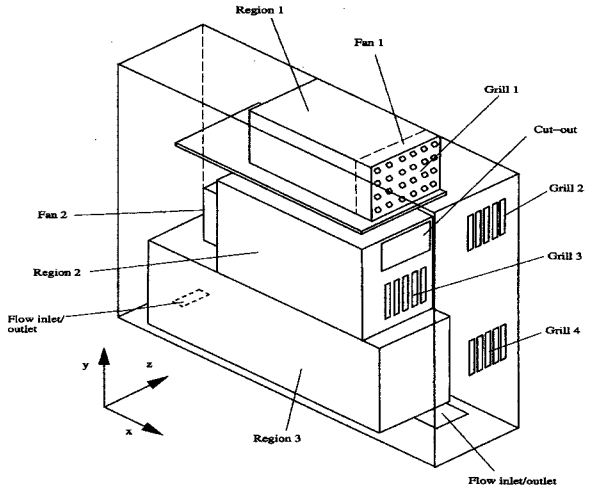

Figure 1: Schematic of flow configuration

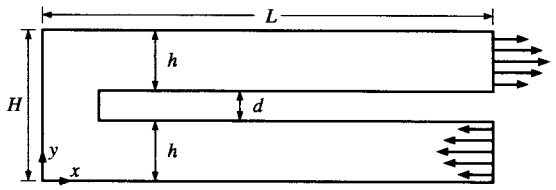

Figure 2: Sharp bend flow configuration.

This yields an expression of the form

$$\sigma_{ij} = \tau_{ij} - 1/3\delta_{ij}\tau_{kk} = -2\nu_t S_{ij}, \tag{4}$$

$$\nu_t = l^2|\overline{S}|, \tag{5}$$

where l is a length scale, and $|\overline{S}| = \sqrt{2S_{ij}S_{ij}}$ is the magnitude of the large-scale strain-rate tensor. In the Smagorinsky model, l can be calculated as follows:

$$l = \min(\kappa y, C_S\Delta), \tag{6}$$

where κ is the von Karman constant and C_S the Smagorinsky constant. Δ is a filter width defined as

$$\Delta = (\Delta_x\Delta_y\Delta_z)^{1/3}. \tag{7}$$

Linear k-l model of Yoshizawa (1993).

In this study, the modified one equation subgrid-scale model of Yoshizawa (1993) is used. The eddy viscosity ν_t is obtained in the following form,

$$\nu_t = C_\mu\Delta k^{1/2}, \tag{8}$$

where $C_\mu = 0.07$.

The transport equation for the SGS energy, k, is given by,

$$\frac{Dk}{Dt} = \frac{\partial}{\partial x_j}\left[(\nu + \nu_t)\frac{\partial k}{\partial x_j}\right] + P_k - \varepsilon_k. \tag{9}$$

Here, P_k and ε_k are production and dissipation terms defined as

$$P_k = 2\nu_t S_{ij}S_{ij}, \tag{10}$$

$$\varepsilon_k = C_e\frac{k^{3/2}}{\Delta}, \tag{11}$$

where, S_{ij} is the strain rate tensor and $C_\varepsilon = 1.05$.

Nonlinear k-l SGS model of Kosović (1997).

The nonlinear subgrid-scale model of Kosović (1997) is also used.

$$\sigma_{ij} = -C_e\Delta\left(2k^{1/2}S_{ij} + \left(\frac{27}{8\pi}\right)^{1/3}C_S^{2/3}\Delta N\right),$$

$$N = \left[C_1\left(S_{ik}S_{kj} - \frac{1}{3}S_{mn}S_{nm}\delta_{ij}\right) + C_2\left(S_{ik}\Omega_{kj} - \Omega_{ik}S_{kj}\right)\right].$$

where

$$S_{ij} = \frac{1}{2}\left(\frac{\partial u_i}{\partial x_j} + \frac{\partial u_j}{\partial x_i}\right), \tag{12}$$

$$\Omega_{ij} = \frac{1}{2}\left(\frac{\partial u_i}{\partial x_j} - \frac{\partial u_j}{\partial x_i}\right). \tag{13}$$

The nonlinear model parameters are determined by first choosing the appropriate backscatter parameter, C_b. Choosing $S(k_c) = 0.5$ and $C_b = 0.36$ gives:

$$C_S = \left[\frac{8(1+C_b)}{27\pi^2}\right]^{1/2} = 0.202061,$$

$$C_1 = \left[\frac{960^{1/2}C_b}{7(1+C_b)S(k_c)}\right]^{1/2} = 1.53078,$$

$$C_2 = C_1 = 1.53078,$$

$$C_e = \left(\frac{8\pi}{27}\right)^{1/3}C_S^{4/3} = 0.115771,$$

$$C_C = C_e\left(\frac{27}{8\pi}\right)^{1/3}C_S^{2/3}C_1 = 0.0625 \approx \frac{1}{16}.$$

Solver

The governing equations are solved using a finite volume method with the Crank-Nicholson scheme. The second-order central difference is used for the convective and viscous terms. The pressure field is produced using the SIMPLE algorithm (Patankar and Spalding, 1972). At inflow and outflow boundaries the total (static + dynamic) pressure is fixed. Appropriate Dirichlet or Neumann boundary conditions are set depending on the flow condition. Fans 1 and 2 are modelled using quadratic momentum sources based on manufacturers characteristic curves. No-slip conditions are applied at solid surfaces. The temperature of the incoming flow is constant at T_i. A heater is located at $y = 0.5$, $0.145 \le x \le 0.265$ and $0.0755 \le z \le 0.1875$, in Region A (see Fig. 3). Constant heater temperature T_w boundary conditions are used. For relevance to heat transfer from circuit boards $T_w > T_i$ and the internal walls are adiabatic. The temperature at the remaining walls is constant at T_i. Details of the boundary conditions can be found in Tucker (2001) and Chung *et al.* (2001). A 105×107×51 grid system is used in the x, y, and z directions, respectively. For unsteady predictions, time steps of $\Delta t = 0.001$ are used.

RESULTS AND DISCUSSION

Channel Flow

First, it is important to ascertain the reliability and accuracy of the present large-eddy simulation. This forms an integral part of the overall validation efforts. Assessment of

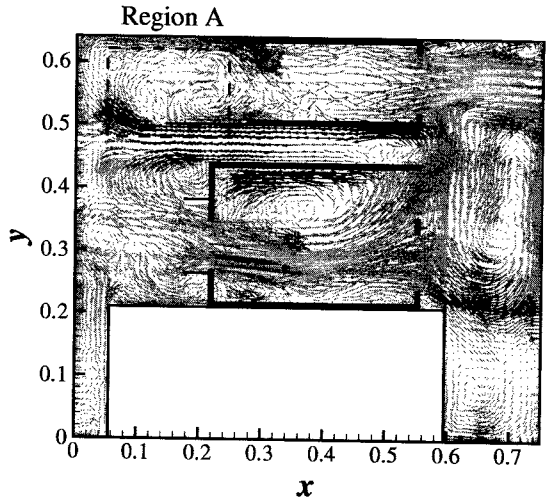

Figure 3: Instantaneous vector plot in x-y plane.

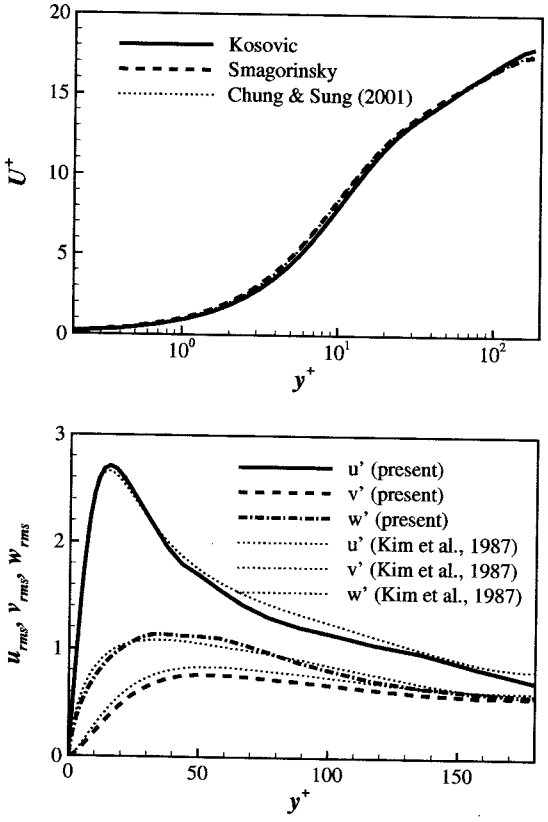

Figure 4: Comparison of time-mean velocity and turbulent intensities in channel flow.

the present simulations is made by comparing the numerical results to well-confirmed data. A fully developed turbulent channel flow with periodic boundary conditions is simulated. The Reynolds number of the channel is $Re_h = 2800$ based on the mean velocity U_m and the channel half-width h. This corresponds to $Re_\tau = 180$, based on the friction velocity u_τ. $3.14h$, respectively. The present results with Kosović (1997) model are shown in Fig. 4. The DNS data of Kim *et al.* (1987) is also included. The mean velocity and turbulence quantities of the present simulation are in close agreement

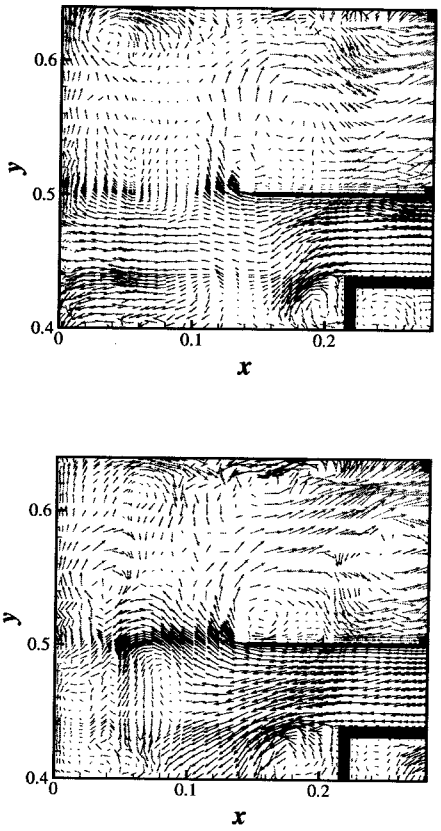

Figure 5: Instantaneous vector plot in x-y plane at two time instants.

with other LES (Chung and Sung, 1997) and DNS (Chung and Sung, 2001) data.

Electronic System Flow Field

The complexity of the flow is clearly seen in Fig. 3, which gives an instantaneous vector plot in an x-y plane. The flow field is characterised by large unsteady vortex structures. Flow separation takes place in several regions. Downstream of Fan 2, two recirculating regions are seen. It is expected that heat transfer is deteriorated in the separation regions. The unsteadiness of the flow in Region A is shown with instantaneous vector plots in Fig. 5. Flow changes significantly in time. It is clear that the size of the separation region changes in time.

Comparisons are made with measurements at six locations. The exact profile locations are shown in Table 1. Figure 6 compares the LES predictions with the time averaged measurements of Tucker and Pan (2001). The LDA measurements have an estimated accuracy of ±5%. For interest Pitot-static tube measurements are also shown. Velocities are normalised by the average axial velocity (U_0). Simulations are performed with Smagorinsky (1963) model, linear Yoshizawa (1993) model and non-linear Kosović (1997) model. The LES results are better than the URANS using the standard k-ϵ model. LES velocity profiles are in good agreement with time averaged LDA measurements.

Electronic System Turbulence Intensities

Figure 7 shows the turbulent kinetic energy and pres-

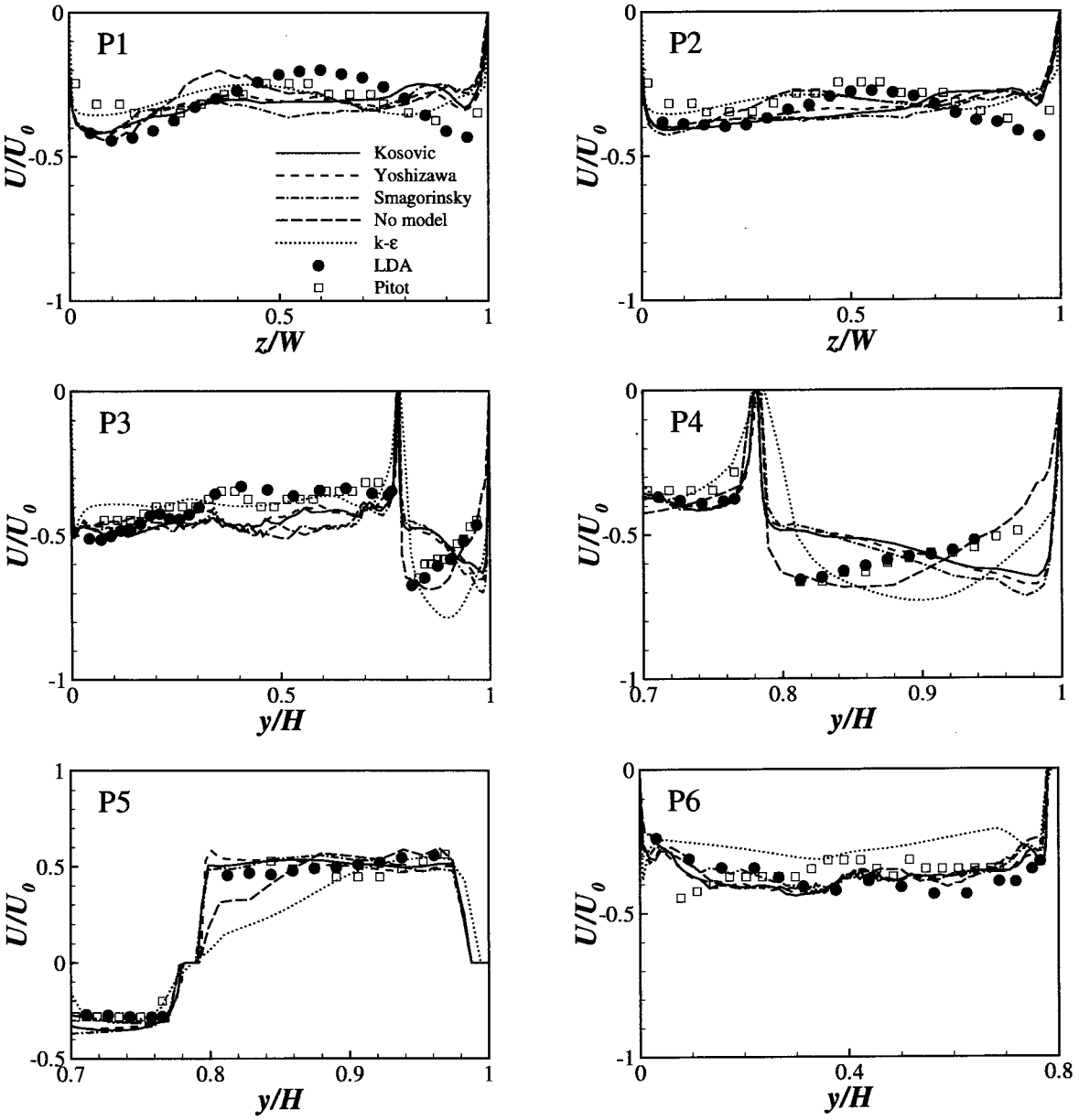

Figure 6: Time-mean velocity (U/U_0) at profiles P1 – P6.

Table 1: Profile locations. Here L, H and W are the maximum extent of system in x, y and z directions, respectively. $L = 0.75, H = 0.64, W = 0.2$.

Profile	x/L	y/H	z/W
P1	0.53	0.73	—
P2	0.37	0.73	—
P3	0.41	—	0.06
P4	0.41	—	0.10
P5	0.37	—	0.57
P6	0.41	—	0.96

sure fluctuation distributions at mid-span in the x-y plane. Highly unsteady flow characteristics are evident in the figure. The overall turbulent kinetic energy is very high, making the URANS simulations difficult (Tucker, 2001). Especially, turbulent kinetic energy is high upstream and downstream of Fan 2 (See Fig. 1). The channel part has relatively low turbulent kinetic energy.

The unsteadiness of the flow is also clearly seen in Fig. 8, which shows the temporal velocity variation at the centre of profile P5. Low frequency oscillations corresponding to large-scale vortical motions are discernible. The fluctuating part of the velocity is significant. The large amplitude oscillations are caused by the flow separation and resulting unsteady vortex structures. It is worth noting that the URANS with the k-ε model gives a steady flow without any unsteady fluctuations (Tucker, 2001).

Turbulence intensities u'/U_0 with measurements are also compared (not shown here). The non-linear one-equation SGS model gives better results compared to the Smagorinsky model. However, the difference is small and the average error is still quite large.

Electronic System Heat Transfer

Time-mean and instantaneous temperature fields are

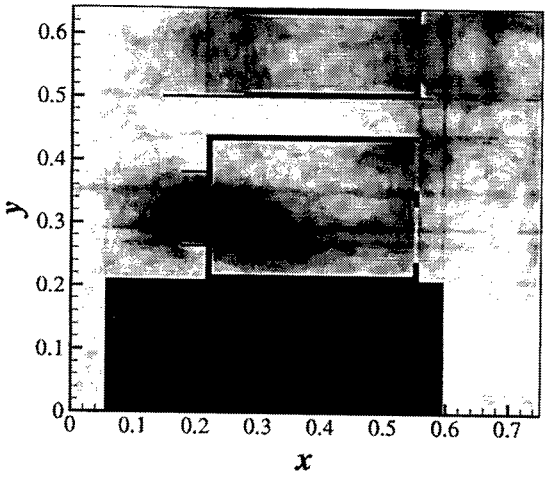

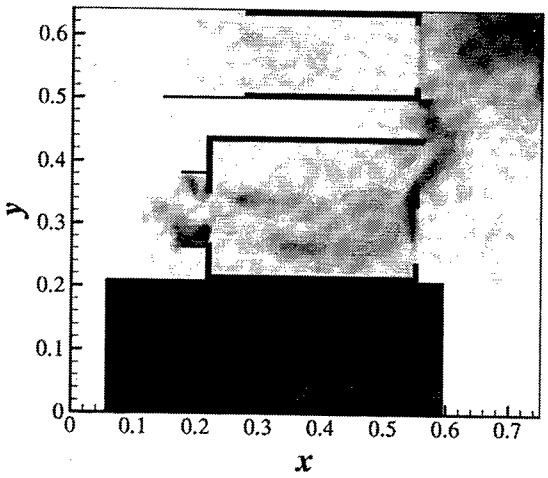

Figure 7: Turbulent kinetic energy (top) and pressure fluctuations (bottom) distributions in x-y plane.

shown in Fig. 9. The convective heat transfer shows strong unsteadiness due to the unsteady flow observed by Chung *et al.* (2001). The flow in Region A, where the heater is located, is similar to the flow around sharp 180° bend. As shown in Fig. 10, temperature fluctuations are high near the heater area. They become smaller in the downstream direction due to the flow mixing.

Time-mean Nusselt number Nu distributions along the surface of the heater are shown in Fig. 11 for the three subgrid-scale models. Nu increases gradually with the downstream direction. It is found that Nu is much higher than in the steady bend flow of Chung *et al.* (2003), indicating that heat transfer has been enhanced by unsteady vortical motions near the corner. Smagorinsky model underpredicts the heat transfer compared to the one-equation models.

CONCLUDING REMARKS

Large-eddy simulations of the turbulent flow and heat transfer inside an electronic system have been performed. Three subgrid-scale models are used: the linear one-equation

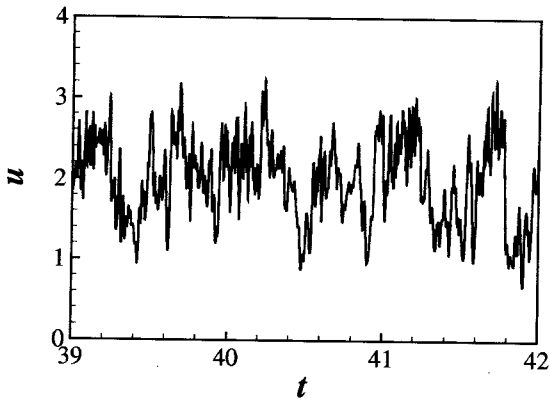

Figure 8: Instantaneous velocity data from profile P5.

subgrid-scale model of Yoshizawa (1993), the non-linear one-equation model of Kosović (1997) model and the Smagorinsky model. The results are compared with Laser Doppler Anemometry (LDA) measurements along with Unsteady Reynolds Averaged Navier-Stokes (URANS) computations. Compared to URANS predictions, the LES results give better agreement with turbulence measurements. The one-equation (linear and non-linear) subgrid-scale models produce better heat transfer results than the Smagorinsky model.

ACKNOWLEDGEMENTS

The support of the Engineering and Physical Sciences Research Council (EPSRC) of the United Kingdom under grant number GR/N05581 is gratefully acknowledged.

REFERENCES

Chung, Y. M., Sung, H. J., 1997, "Comparative study of inflow conditions for spatially evolving simulation", *AIAA J.*, Vol. 35, pp. 269–274.

Chung, Y. M., Sung, H. J., 2001, "Initial relaxation of spatially evolving turbulent channel flow with blowing and suction", *AIAA J.*, Vol. 39, pp. 2091–2099.

Chung, Y. M., Tucker, P. G., Luo, K. H., 2001, "Large-eddy simulation of complex internal flows", *Direct and Large-Eddy Simulation IV*, B. J. Geurts et al., ed., Kluwer Academic Publishers, The Netherlands, pp. 373–380.

Chung, Y. M., Tucker, P. G., Roychowdhury, D. G., 2003, "Unsteady laminar flow and convective heat transfer in a sharp 180° bend", *Int. J. Heat Fluid Flow*, Vol. 24, pp. 67–76.

Ferziger, J. H., 1993, *Large-Eddy Simulation of Complex Engineering and Geophysical Flows*, B. Galperin and S. A. Orszag, ed., Cambridge University Press, New York, pp. 19–33.

Ghaddar, N. K., Karczak, K. Z., Mikic, B. B., and Patera, A. T., 1986a, "Numerical investigation of incompressible flow in grooved channels, Part 1. Stability and self-sustained oscillations", *J. Fluid Mech.*, Vol. 163, pp. 99–127.

Ghaddar, N. K., Magen, M., Mikic, B. B., and Patera, A. T., 1986b, "Numerical investigation of incompressible flow in grooved channels. part 2. Resonance and oscillatory heat-transfer enhancement", *J. Fluid Mech.*, Vol. 168, pp. 541–567.

Jiménez, J., and Moser, R. D., 2000, "Large-eddy simu-

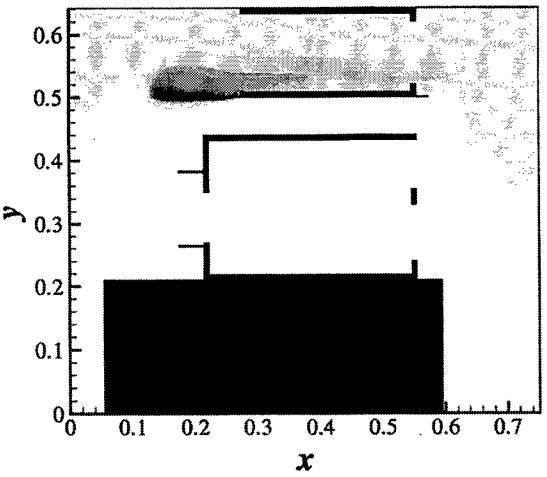

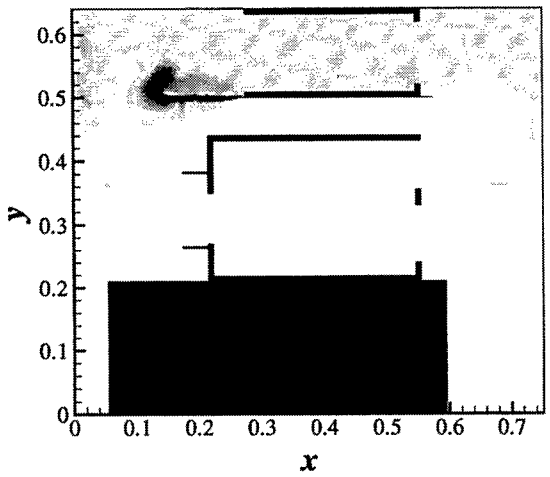

Figure 9: Time-mean (top) and instantaneous (bottom) temperature fields in x-y plane with Yoshizawa (1993) model.

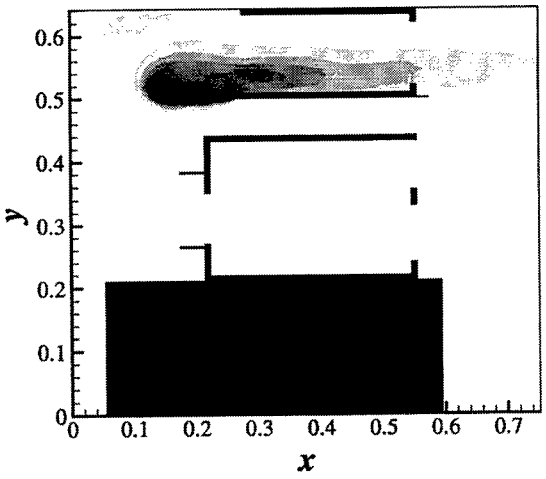

Figure 10: Temperature fluctuations in x-y plane with Yoshizawa (1993) model.

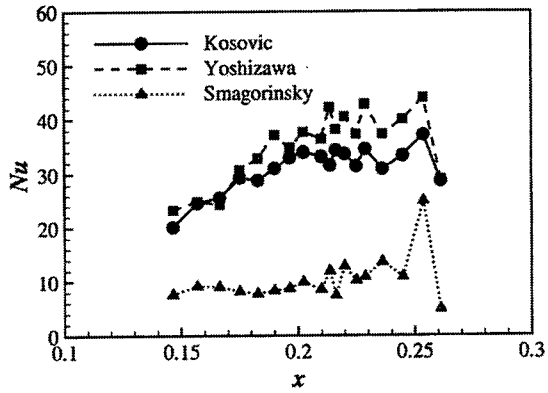

Figure 11: Nu at the heater surface.

lations: Where are we and what can we expect?", *AIAA J.*, Vol. 38, pp. 605–612.

Kim, S. Y., Kang, B. H., and Hyun, J. M., 1997, "Forced convection heat transfer from two heated blocks in pulsating channel flow", *Int. J. Heat Mass Transfer*, Vol. 41, pp. 625–634.

Kosović, B., 1997, "Subgrid scale modelling for the large eddy simulation of high Reynolds number boundary layers", *J. Fluid Mech.*, Vol. 336, pp. 151–182.

Lesieur, M., and Métais, O., 1996, "New trends in large-eddy simulations of turbulence", *Ann. Rev. Fluid Mech.*, Vol. 28, pp. 45–82.

Patankar, S. V., and Spalding, D. B., 1972, "A calculation procedure for heat, mass and momentum transfer in three-dimensional parabolic flows", *Int. J. Heat Mass Transfer*, Vol. 15, pp. 1787–1806.

Patera, A. T., Mikic, B. B., 1986, "Exploiting hydrodynamic instabilities. Resonant heat transfer enhancement", *Int. J. Heat Mass Transfer*, Vol. 29, pp. 1127–1138.

Rodi, W., Ferziger, J. H., Breuer, M., and Pourquié, M., 1997, "Status of large eddy simulation: Results of a workshop", *J. Fluids Engrg.*, Vol. 119, pp. 248–262.

Rollet-Miet, P., Laurence, D., and Ferziger, J. H., 1999, "LES and RANS of turbulent flow in tube bundles", *Int. J. Heat Fluid Flow*, Vol. 20, pp. 241–254.

Smagorinsky, J., 1963, "General circulation experiments with the primitive equations, Part I: The basic experiment", *Monthly Weather Review*, Vol. 91, pp. 99-164.

Spalart, P. R., 2000, "Strategies for Turbulence Modelling and Simulations", *Int. J. Heat Fluid Flow*, Vol. 21, pp. 252–263.

Tucker, P. G., 2001, *Computation of unsteady internal flows*, Kluwer Academic Publishers,

Tucker, P. G., Liu, Y., Chung, Y. M., and Jouvray, A., 2003, "Computation of an unsteady complex geometry flow using novel non-linear turbulence models", *Int. J. Numer. Meth. Fluids*, accepted.

Tucker, P. G., and Pan, Z., 2001, "URANS computations for a complex internal isothermal flow", *Computer Methods in Applied Mechanics and Engineering*, Vol. 190, pp. 2893–2907.

Yoshizawa, A., 1993, "Bridging between eddy-viscosity-type and second-order models using a two-scale DIA", *9th International Symposium on Turbulence Shear Flow*, Vol. 3, pp. 23.1.1–23.1. 6.